

# Online Poisoning Attacks Against Data-Driven Predictive Control

Yue Yu, Ruihan Zhao, Sandeep Chinchali, and Ufuk Topcu

**Abstract**—Data-driven predictive control (DPC) is a feedback control method for systems with unknown dynamics. It repeatedly optimizes a system’s future trajectories based on past input-output data. We develop a numerical method that computes poisoning attacks that inject additive perturbations to the online output data to change the trajectories optimized by DPC. This method is based on implicitly differentiating the solution map of the trajectory optimization in DPC. We demonstrate that the resulting attacks can cause an output tracking error one order of magnitude higher than random perturbations in numerical experiments.

## I. INTRODUCTION

Data-driven predictive control (DPC) is a feedback control method for systems with unknown dynamics [1], [2], [3]. It combines the idea of Willems’ fundamental lemma and model predictive control: the former gives a parameterization of the system’s future input-output trajectories using linear functions of the past input-output data [4], [5], [6], and the latter gives a feedback controller that repeatedly optimizes the system’s future input-output trajectories [7], [8]. DPC has been successful for various systems, including quadrotors [9], power converters [10], as well as building heating, ventilation, and air conditioning [11].

Since DPC relies heavily on data, it is susceptible to adversarial data perturbations, or *data poisoning attacks* [12], [13], [14], [15]. On the other hand, it remains unclear how vulnerable DPC is against data poisoning attacks. The results in [16], [17] show that DPC is robust against zero-mean stochastic noise in data. But they do not extend to deterministic data poisoning attacks. Meanwhile, results on data poisoning attacks against state estimators [18], [19], [20], [21] and virtual reference feedback controllers [22], [23] do not consider DPC, or any trajectory-optimization-based controllers. To our best knowledge, data poisoning attacks against DPC have received little if any attention.

We formulate a data-poisoning attack problem in DPC, where an *attacker* computes bounded additive perturbations to the online output data—which lack the thorough validation typically available for offline data and, compared with input data, are sensitive to noninvasive modifications of the sensors’ physical environment [18]—to change the trajectories optimized by DPC. We show that computing a poisoning attack is a bilevel optimization: the lower level optimizes the trajectory in DPC, and the upper level optimizes the attack.

Y. Yu, R. Zhao, and U. Topcu are with the Oden Institute for Computational Engineering and Sciences, The University of Texas at Austin, TX, 78712, USA (emails: yueyu@utexas.edu, ruihan.zhao@utexas.edu, utopcu@utexas.edu). S. Chinchali is with the Department of Electrical and Computer Engineering, The University of Texas at Austin, TX, 78712, USA (email: sandeepc@utexas.edu).

Furthermore, we develop an efficient numerical method to compute poisoning attacks against DPC by approximating the bilevel optimization using a single-level convex optimization. We construct this approximation in two steps. First, we transform the bilevel optimization into a single-level nonconvex optimization using the solution map of the lower-level trajectory optimization. Second, we approximate the single-level nonconvex optimization using a convex one by implicitly differentiating said solution map.

Finally, we demonstrate the effectiveness and efficiency of the proposed method in attacking DPC for a linear oscillating masses system and a nonlinear quadrotor system in PyBullet, a high-fidelity robotics simulator [24]. Our numerical experiments show that the performance of DPC is more sensitive to data-poisoning attacks than random noise: the former can cause an output tracking error one order of magnitude higher than that of the latter. Furthermore, the proposed method is more efficient in implicit differentiation than CVXPYlayers, a state-of-the-art differentiation toolbox [25]. In our experiments, the least-squares problem solved in the proposed method—which is the main computational task in implicit differentiation—is about half the size of the one solved in CVXPYlayers.

Our work complements the qualitative results in robust DPC. Although regularization can qualitatively stabilize DPC against data perturbations [26], [27], how to quantitatively compute the regularization parameters is, to our best knowledge, still an open question. Our results enable quantitative evaluation and potentially automated search of these regularization parameters based on their stabilizing performance under poisoning attacks.

*Notation:* We let  $\mathbb{R}$ ,  $\mathbb{R}_+$ ,  $\mathbb{R}_{++}$ , and  $\mathbb{N}$  denote the set of real, nonnegative real, positively real, and positive integer numbers, respectively. Given  $m, n \in \mathbb{N}$ , we let  $\mathbb{R}^n$  and  $\mathbb{R}^{m \times n}$  denote the set of  $n$ -dimensional real vectors and  $m \times n$  real matrices, We let  $0_n$  and  $I_n$  denote the  $n$ -dimensional zero vector and the  $n \times n$  identity matrix, respectively. Given a square real matrix  $A \in \mathbb{R}^{n \times n}$ , we let  $A^\top$ ,  $A^{-1}$ , and  $A^\dagger$  denote the transpose, the inverse, and the Moore–Penrose inverse of matrix  $A$ , respectively. Given a symmetric and positive semidefinite matrix  $M \in \mathbb{R}^{n \times n}$  and  $x \in \mathbb{R}^n$ , we let  $\|x\| := \sqrt{x^\top x}$  and  $\|x\|_M := \sqrt{x^\top M x}$ . We let  $\partial G(x) \in \mathbb{R}^{m \times n}$  denote the Jacobian matrix of function  $G$  evaluated at  $x \in \mathbb{R}^n$ . We say a closed set  $\mathbb{D} \subset \mathbb{R}^n$  is a closed convex set if  $\alpha x + (1 - \alpha)y \in \mathbb{D}$  for all  $x, y \in \mathbb{D}$  and  $\alpha \in [0, 1]$ . The *projection* of  $x \in \mathbb{R}^n$  onto a closed convex set  $\mathbb{D} \subset \mathbb{R}^n$  is a function  $\Pi_{\mathbb{D}} : \mathbb{R}^n \rightarrow \mathbb{D}$  where  $\Pi_{\mathbb{D}}(x) := \operatorname{argmin}_{x' \in \mathbb{D}} \|x' - x\|$ .

## II. ONLINE POISONING ATTACK PROBLEM IN DATA-DRIVEN PREDICTIVE CONTROL

We introduce the data poisoning attack problem in data-driven predictive control (DPC). We will first revisit the basics of DPC, then introduce a bilevel optimization that models of data poisoning attacks against DPC.

### A. Data-driven predictive control

We will briefly review the basics of data-driven predictive control, a control law for unknown dynamical systems based on data and optimization.

1) *Input and output trajectories*: Consider a discrete time dynamical system with  $n_u$  inputs and  $n_y$  outputs. The system's input and output at time  $j \in \mathbb{N}$  are denoted by  $u_j \in \mathbb{R}^{n_u}$  and  $y_j \in \mathbb{R}^{n_y}$ , respectively.

At each sampling time  $k$ , DPC requires the knowledge of an online input-output trajectories generated by the system, denoted by  $\{u_{k-\sigma}, \dots, u_{k-1}\}$  and  $\{y_{k-\sigma}, \dots, y_{k-1}\}$ , where  $\sigma \in \mathbb{N}$  is the upper bound of the lag of the system [1]. Intuitively,  $\sigma$  is the number of input-output pairs needed to pinpoint the state of the system. In addition, DPC also requires the knowledge of the input Hankel matrix  $U \in \mathbb{R}^{(\ell+\sigma)n_u \times n_g}$  and output Hankel matrix  $Y \in \mathbb{R}^{(\ell+\sigma)n_y \times n_g}$ , where  $\ell \in \mathbb{N}$  is the planning horizon in DPC, and  $n_g \in \mathbb{N}$  is determined by the amount of offline data. See [5], [6] for a detailed discussion on constructing Hankel matrices using offline input-output trajectories.

2) *Data-driven trajectory optimization*: We now introduce the trajectory optimization problem used in data-driven predictive control. To this end, we first introduce the following notation:

$$u_{\text{ini}} := \begin{bmatrix} u_{k-\sigma} \\ \vdots \\ u_{k-1} \end{bmatrix}, y_{\text{ini}} := \begin{bmatrix} y_{k-\sigma} \\ \vdots \\ y_{k-1} \end{bmatrix}, \begin{bmatrix} U_p \\ U_f \end{bmatrix} = U, \begin{bmatrix} Y_p \\ Y_f \end{bmatrix} = Y, \quad (1)$$

where  $U_p \in \mathbb{R}^{\sigma n_u \times n_g}$  and  $U_f \in \mathbb{R}^{(\ell n_u \times n_g)}$  are partitions of  $U$ ,  $Y_p \in \mathbb{R}^{\sigma n_y \times n_g}$  and  $Y_f \in \mathbb{R}^{(\ell n_y \times n_g)}$  are partitions of  $Y$ .

At each discrete time  $k \in \mathbb{N}$ , the data-driven predictive controller computes a length- $\ell$  future input and output trajectory of the system—denoted by  $u := [u_k^\top \ u_{k+1}^\top \ \dots \ u_{k+\ell-1}^\top]^\top$  and  $y := [y_k^\top \ y_{k+1}^\top \ \dots \ y_{k+\ell-1}^\top]^\top$ , respectively—by solving the following optimization problem:

$$\begin{aligned} \text{minimize}_{u, y, g} \quad & \frac{1}{2} \|y - \hat{y}\|_Q^2 + \frac{1}{2} \|u - \hat{u}\|_R^2 + \lambda_g \|Mg\|^2 \\ & + \lambda_s \|Y_p g - y_{\text{ini}}\|^2 \\ \text{subject to} \quad & u_{\text{ini}} = U_p g, u = U_f g, y = Y_f g, u \in \mathbb{U}, y \in \mathbb{Y}. \end{aligned} \quad (2)$$

where  $M := I_{n_g} - \begin{bmatrix} U_p \\ Y_p \\ U_f \end{bmatrix}^\dagger \begin{bmatrix} U_p \\ Y_p \\ U_f \end{bmatrix}$  is a weighting matrix inspired by system identification and has proven to be more effective than identity weighting [3]; matrix  $Q \in \mathbb{R}^{\ell n_y \times \ell n_y}$  and matrix  $R \in \mathbb{R}^{\ell n_u \times \ell n_u}$  are both symmetric and positive semidefinite;  $\lambda_g, \lambda_s \in \mathbb{R}_+$  are regularization weights; set  $\mathbb{U} \subset \mathbb{R}^{\ell n_u}$  and set  $\mathbb{Y} \subset \mathbb{R}^{\ell n_y}$  are the feasible set of input and output trajectories, respectively;  $\hat{u} \in \mathbb{R}^{\ell n_u}$  and  $\hat{y} \in \mathbb{R}^{\ell n_y}$  are the reference input and output trajectory in DPC, respectively. The constraints and objective function in

optimization (2) ensures that  $\begin{bmatrix} u_{\text{ini}} \\ u \end{bmatrix} = \begin{bmatrix} U_p \\ U_f \end{bmatrix} g$  and  $\begin{bmatrix} y_{\text{ini}} \\ y \end{bmatrix} \approx \begin{bmatrix} Y_p \\ Y_f \end{bmatrix} g$ , which says all trajectories are approximately linear functions of past data.

### B. Poisoning attacks against data-driven predictive control

We consider a scenario where the online output measurements in optimization (2) are corrupted by bounded additive perturbations designed by a malicious attacker. To this end, we start with the following variation of optimization (2):

$$\begin{aligned} \text{minimize}_{u, y, g} \quad & \frac{1}{2} \|y - \hat{y}\|_Q^2 + \frac{1}{2} \|u - \hat{u}\|_R^2 + \lambda_g \|Mg\|^2 \\ & + \lambda_s \|Y_p g - (y_{\text{ini}} + p)\|^2 \\ \text{subject to} \quad & u_{\text{ini}} = U_p g, u = U_f g, y = Y_f g, u \in \mathbb{U}, y \in \mathbb{Y}, \end{aligned} \quad (3)$$

where  $p \in \mathbb{R}^{\sigma n_y}$  is an attacking perturbation. Notice that optimization (2) is a special case of optimization (3) if  $p = 0_{\sigma n_y}$ . We focus on attacks against the online output data in vector  $y_{\text{ini}}$ . Unlike the offline data in matrix  $Y_p$  and  $Y_f$ , these data are generated in real-time and are more likely to lack thorough validation. Unlike input data, they are sensitive to noninvasive modification of sensors' physical environment, even when properly encrypted [18].

We now introduce the poisoning attack problem against data-driven predictive control, where an attacker seeks the optimal bounded perturbation  $p$  such that the optimal input trajectory in optimization (3) minimizes a performance function chosen by the attacker. We summarize the definition of this poisoning attack problem as follows.

**Definition 1** (Poisoning attack problem). *Given optimization (3), a continuously differentiable cost function  $\psi : \mathbb{R}^{\ell n_u} \rightarrow \mathbb{R}$  that evaluates the performance of the attacked trajectory, and a closed convex set  $\mathbb{P} \subset \mathbb{R}^{\sigma n_y}$  for admissible attacking perturbations, the poisoning attack problem seeks the optimal perturbation vector  $p \in \mathbb{P}$  in the following bilevel optimization problem:*

$$\begin{aligned} \text{minimize}_{u, y, g, p} \quad & \psi(u) \\ \text{subject to} \quad & p \in \mathbb{P}, [u^\top \ y^\top \ g^\top]^\top \text{ is optimal for (3)}. \end{aligned} \quad (4)$$

As an example of problem (4), one can let

$$\psi(u) = \frac{1}{2} \|u - \tilde{u}\|^2, \quad \mathbb{P} = \{p \in \mathbb{R}^{\sigma n_y} \mid \|p\| \leq \rho \|y_{\text{ini}}\|\}, \quad (5)$$

where  $\tilde{u}$  is the attacker's desired input trajectory, and  $\rho \in \mathbb{R}_+$  is the ratio between the norm of the attacking perturbation and the output measurements. In this case, the attacker aims to push the input trajectory computed by DPC towards  $\tilde{u}$  by adding a perturbation  $p$ , where the perturbation-to-data ratio is upper bounded by  $\rho$ . By choosing different values of  $\rho$ , one can evaluate the effects of different attacks against DPC by solving optimization (4).

We assume that the attacker's objective function only depends on the input trajectory  $u$  and that it has full knowledge of the parameters in optimization (2) (such as  $\lambda_s$  and  $\lambda_g$ ). The former assumption is because DPC uses only the input trajectory  $u$  to construct the input to the system [1, Alg.

2]. The output trajectory  $y$ , on the other hand, is merely a computational byproduct during this construction. The latter assumption ensures that problem (3) gives the worst-case estimate of the attacker's perturbations.

If the underlying system is linear time-invariant and the output data are the state data, then, due to Willems' lemma [4], [5], [6], problem (3) is equivalent to the attacking of model predictive control. However, problem (3) also applies to nonlinear systems and systems without state data.

### III. POISONING ATTACKS VIA IMPLICIT DIFFERENTIATION

We introduce an efficient numerical method to approximately solve the bilevel optimization problem in (4). Our method is based on the implicit function theorem [28, Thm. 1B.1] and a novel form of optimality conditions based on the Minty parameterization theorem [29, Prop. 23.22].

To simplify our notation in this section, we will first rewrite trajectory optimization (3) in a compact form. To this end, we introduce the following notation:

$$\begin{aligned} m &= \ell(n_u + n_y) + \sigma n_u, \quad n = \ell(n_u + n_y) + n_g, \\ z &= [u^\top \quad y^\top \quad g^\top]^\top, \quad \mathbb{D} = \mathbb{U} \times \mathbb{Y} \times \mathbb{R}^{n_g}, \\ P &= \text{blkdiag}(R, Q, 2\lambda_g M^\top M + 2\lambda_s Y_p^\top Y_p), \\ q(p) &= -[R\hat{u}^\top \quad Q\hat{y}^\top \quad 2\lambda_s(p + y_{\text{ini}})^\top Y_p]^\top, \\ H &= \begin{bmatrix} 0_{\sigma n_u \times \ell n_u} & 0_{\sigma n_u \times \ell n_y} & U_p \\ -I_{\ell n_u} & 0_{\ell n_u \times \ell n_y} & U_f \\ 0_{\ell n_y \times \ell n_u} & -I_{\ell n_y} & Y_f \end{bmatrix}, \quad b = \begin{bmatrix} u_{\text{ini}} \\ 0_{\ell(n_u + n_y)} \end{bmatrix}, \end{aligned} \quad (6)$$

where  $P$  is the block diagonal matrix obtained by aligning  $R, Q, 2\lambda_g M^\top M + 2\lambda_s Y_p^\top Y_p$  along its diagonal.

With the above notation, we can rewrite optimization (3) in the following form:

$$\begin{aligned} &\underset{z}{\text{minimize}} \quad \frac{1}{2} z^\top P z + q(p)^\top z \\ &\text{subject to} \quad H z = b, \quad z \in \mathbb{D}. \end{aligned} \quad (7)$$

Next, we will work with the compact notation in (7), rather than (3); we remind the readers again that the two are exactly equivalent due to (6).

Throughout, we will make the following assumption on optimization (7).

**Assumption 1.** *Set  $\mathbb{D} \subseteq \mathbb{R}^n$  is closed and convex. There exists  $z^* \in \mathbb{R}^n$  and  $w^* \in \mathbb{R}^m$  such that*

$$z^* \in \underset{z \in \mathbb{D}}{\text{argmin}} L(z, w^*), \quad w^* \in \underset{w}{\text{argmax}} L(z^*, w), \quad (8)$$

where  $L(z, w) := \frac{1}{2} z^\top P z + q(p)^\top z + w^\top (H z - b)$ .

Under mild constraint qualification conditions on optimization (7) [30, Cor. 28.3.1], (8) holds if and only if there exists an optimal solution for optimization (7).

We are interested in how the perturbation vector  $p$  affects the optimal solutions of optimization (7). To this end, we introduce the following definition, which characterizes the mathematical relations between the two.

**Definition 2** (Solution map and its localization). *The solution map of optimization (7) is denoted by  $S : p \mapsto S(p)$  where  $S(p) := \{[(z^*)^\top \quad (w^*)^\top]^\top \mid \text{Conditions in (8) hold}\}$ . We say solution map  $S$  has a single-valued localization around  $p$  if there exists a function  $\tilde{S}$  such that  $\tilde{S}(\tilde{p}) \in S(\tilde{p})$  for all  $\tilde{p}$  in a neighborhood of  $p$ .*

In the following, we will discuss the differentiability properties of solution map  $S$  and its localization.

#### A. Optimality conditions as nonlinear equations

The implicit function theorem provides a characterization of the Jacobian of the solution maps of nonlinear equations [28, Thm. 1B.1]. On first look, the implicit function theorem seems not applicable to the solution map  $S$  in Definition 2, since the latter is defined by an optimization problem rather than nonlinear equations. However, the following proposition shows that the optimality conditions in (8) are actually equivalent to a set of nonlinear equations, laying the groundwork for applying the implicit function theorem to the solution map  $S$ .

**Lemma 1.** *Let*

$$F\left([z^\top \quad w^\top]^\top, p\right) := \begin{bmatrix} z - \Pi_{\mathbb{D}}(z - Pz - q(p) - H^\top w) \\ Hz - b \end{bmatrix},$$

for all  $z \in \mathbb{R}^n$  and  $w \in \mathbb{R}^m$ . Then the conditions in (8) are equivalent to the following conditions:

$$F\left([z^*]^\top \quad [w^*]^\top\right)^\top, p = 0_{m+n}. \quad (9)$$

*Proof.* First, the conditions in (8) are equivalent to the following [30, Thm. 27.4]:

$$Pz^* + q(p) + H^\top w^* + N_{\mathbb{D}}(z^*) \ni 0_n, \quad Hz^* - b = 0_m. \quad (10)$$

where  $N_{\mathbb{D}}(z^*)$  is the normal cone of set  $\mathbb{D}$  at  $z^*$ . Next, since the set  $\mathbb{D}$  is nonempty, closed, and convex,  $N_{\mathbb{D}}$  is a maximal monotone operator [29, Ex. 20.26]. The rest of the proof follows directly from the Minty parameterization theorem for maximal monotone operators [29, Prop. 23.22].  $\square$

Lemma 1 shows that the optimizers in (8) are the fixed-points of the *proportional integral projected gradient method*, a first-order primal-dual conic optimization method that combines gradient descent with proportional-integral feedback [31], [32], [33].

**Remark 1.** *Compared with the results in [25], the optimality conditions in Lemma 1 contain fewer variables by eliminating dual variables for any inequality constraints.*

#### B. Implicit differentiation through optimality conditions

Equipped with Lemma 1, we are ready to present the differentiability properties of the solution map in Definition 2 as follows.

**Proposition 1** (Implicit function theorem). *Consider the solution mapping  $S$  in Definition 2. Suppose Assumption 1 holds and  $z^+ := z^* - Pz^* - q - H^\top w^*$ . In addition,*

suppose function  $\Pi_{\mathbb{D}}$  is continuously differentiable within a neighborhood of  $z^+$ . Let

$$\begin{aligned} J &:= \begin{bmatrix} I_n - \partial\Pi_{\mathbb{D}}(z^+)(I_n - P) & \partial\Pi_{\mathbb{D}}(z^+)H^\top \\ H & 0_{m \times m} \end{bmatrix}, \\ K &:= \begin{bmatrix} \partial\Pi_{\mathbb{D}}(z^+) \begin{bmatrix} 0_{\sigma n_y \times (\ell n_u + \ell n_y)} & -2\lambda_s Y_p \end{bmatrix}^\top \\ 0_{m \times \sigma n_y} \end{bmatrix}. \end{aligned} \quad (11)$$

If matrix  $J$  is nonsingular, the solution map  $S$  has a single-valued localization  $\tilde{S}$ . Within a neighborhood of  $p$ , function  $\tilde{S}$  is continuously differentiable with its Jacobian satisfying:

$$\partial\tilde{S}(p) = -J^{-1}K. \quad (12)$$

*Proof.* Our proof is based on the implicit function theorem [28, Thm. 1B. 1]. To use this theorem, let  $\xi \in \mathbb{R}^{m+n}$  be arbitrary and consider the nonlinear equations  $F(\xi, p) = 0_{m+n}$  in (9) and the Jacobian  $\partial_\xi F(\xi, p)$  and  $\partial_p F(\xi, p)$ . Using the chain rule we can show that  $\partial_\xi F(\xi, p) = J$  and  $\partial_p F(\xi, p) = K$ , where  $J$  and  $K$  are given in (11). The rest of the proof is a direct application of the implicit function theorem [28, Thm. 1B. 1].  $\square$

**Remark 2.** Proposition 1 assumes the local differentiability of function  $\Pi_{\mathbb{D}}$ . This assumption holds almost everywhere if set  $\mathbb{U}$  and  $\mathbb{Y}$  are Cartesian products of many common closed convex cones; see [34, Sec. 3] for an overview. If these sets are intervals, then  $\Pi_{\mathbb{D}}$  is piecewise-linear [35, Thm. 3.3.14] and also differentiable almost everywhere.

### C. Poisoning attacks via implicit differentiation

We now introduce the *approximate poisoning attack problem*, where we approximate the bilevel optimization in (4) via linearization and implicit differentiation.

Due to Definition 2, we know that  $z \in \mathbb{R}^n$  is optimal for (4) if and only if there exists  $w \in \mathbb{R}^m$  such that  $[z^\top \ w^\top]^\top \in S(p)$ . Hence  $[u^\top \ y^\top \ g^\top]^\top$  is optimal for optimization (4) if and only if  $u \in TS(p)$ , where  $T = [J\ell_{n_u} \ 0_{\ell n_u \times (m+n-\ell n_u)}]$ . Therefore, we can rewrite optimization (4) equivalently as the following one:

$$\underset{p \in \mathbb{P}}{\text{minimize}} \quad \psi(TS(p)). \quad (13)$$

Second, suppose that the assumptions in Proposition 1 hold when  $p = 0_{\sigma n_y}$ . Then, there exists unique  $\xi^* := [(z^*)^\top \ (w^*)^\top]^\top \in \mathbb{R}^{m+n}$  such that  $\xi^* = \tilde{S}(0_{m+n})$ , where  $\tilde{S}$  is the single-valued localization of  $S$  around  $0_{\sigma n_y}$ . Due to the chain rule and Proposition 1, the following approximation based on Talor series holds for all  $p \approx 0_{\sigma n_y}$ :

$$\psi(TS(p)) = \psi(T\tilde{S}(p)) \approx \psi(T\xi^*) - \partial\psi(T\xi^*)TJ^{-1}Kp, \quad (14)$$

where matrix  $J$  and  $K$  are given by (11) with

$$q = -[R\hat{u}^\top \ Q\hat{y}^\top \ 2\lambda_s y_{\text{ini}}^\top Y_p]^\top. \quad (15)$$

In other words, we let  $p = 0_{\sigma n_y}$  in (6).

By substituting the linear approximation in (14) into optimization (13), we obtain the following *approximate poisoning attack problem*:

$$\underset{p \in \mathbb{P}}{\text{minimize}} \quad -\partial\psi(T\xi^*)TJ^{-1}Kp \quad (16)$$

---

### Algorithm 1 Poisoning attack via implicit differentiation

---

**Input:** The parameters in optimization (7).

- 1: Solve optimization (7) with  $p = 0_{\sigma n_y}$  for  $z^*$  and  $w^*$  such that  $\xi^* = [(z^*)^\top \ (w^*)^\top]^\top$  and  $F(\xi^*, 0_{\sigma n_y}) = 0_{m+n}$ .
- 2: Compute  $J$  and matrix  $K$  using (11) with  $p = 0_{\sigma n_y}$ .
- 3:  $p^* \in \underset{z \in \mathbb{P}}{\text{argmin}} -\partial\psi(T\xi^*)TJ^{-1}Kp$ .

**Output:** Perturbation  $p^*$ .

---

Based on the observations above, we present Algorithm 1 for computing an approximate solution to the poisoning attack problem in Definition 1. Notice that, since matrix  $J$  in (16) can be singular—or ill-conditioned—we approximate the matrix inverse in (16) with the corresponding Moore–Penrose pseudoinverse in line 3. Evaluating this approximation requires solving a least-squares problem, which is common in implicit differentiation [25].

Using Algorithm 1, one can approximately solve bilevel optimization (4), which is NP-hard to solve exactly [36]. Implementing Algorithm 1 only requires solving the convex trajectory optimization problem in (7), a least-squares problem, and the minimization of a linear function over set  $\mathbb{P}$ . Furthermore, Proposition 1 ensures that, under certain local differentiability and nonsingularity assumptions, Algorithm 1 gives the optimal solution of a linear approximation of the bilevel optimization in (4).

## IV. NUMERICAL EXPERIMENTS

We demonstrate the effectiveness of the perturbations computed by Algorithm 1 in the attacking of two different dynamical systems: a linear oscillating masses system, a popular benchmark linear system in optimal control [32], and the nonlinear quadrotor dynamics in robotics simulator PyBullet [24].

### A. DPC trajectory optimization setup

Furthermore, based on the observations made in DPC literature [9], [3], we choose  $n_g = 500$ ,  $\sigma = 6$ ,  $\ell = 25$ ,  $\lambda_s = 10^6$ , and  $\lambda_g = 100$  in optimization (3). Throughout we solve optimization (3) using ECOS [37] with these parameters. We consider the following two systems.

a) *Oscillating masses system:* We consider the following oscillating-masses system:

$$x_{k+1} = \exp(\Delta A)x_k + \int_0^\Delta \exp(sA) ds Bu_k, \quad y_k = x_k,$$

where  $A = \begin{bmatrix} 0 & 0 & 1 & 0 \\ 0 & 0 & 0 & 1 \\ -2 & 1 & 0 & 0 \\ 1 & -2 & 0 & 0 \end{bmatrix}$ ,  $B = \begin{bmatrix} 0 & 0 \\ 0 & 0 \\ 1 & 0 \\ 0 & 1 \end{bmatrix}$ ,  $\exp$  denotes the matrix exponential, and  $\Delta = 0.1$  is the sampling time period. This system has  $n_u = 2$  and  $n_y = 4$ , and describes the dynamics of two unit masses connected by springs with unit spring constants; see Fig. 1 for an illustration. When

solving optimization (3) with this system, we let  $Q = 10I_4$ ,  $R = I_2$ , and  $\hat{y}$  denote the stationary point with positive unit displacement (see Fig. 3 for an illustration). We choose  $\mathbb{U}$  and  $\mathbb{Y}$  in (3) such that the input and output are elementwise bounded within the interval  $[-1, 1]$  and  $[-5, 5]$ , respectively.

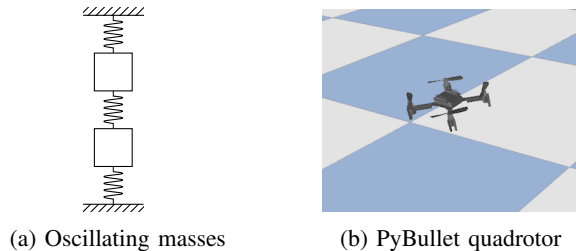


Fig. 1: The two systems controlled by DPC.

*b) PyBullet quadrotor system:* We also consider the nonlinear quadrotor system in PyBullet [24]. This system does not have an explicit description via differential equations. Instead, it is a black-box system composed of pre-tuned PID controllers and 6-degree-of-freedom (6DoF) quadrotor dynamics; see Fig. 2 for an illustration. The input of the system is a 3-dimensional velocity command vector, and the output of the system is a 6-dimensional vector containing the position and orientation angles of the quadrotor. Both input and output are measured at every 0.04 second. When solving optimization (3) with this system, we let  $Q = \text{blkdiag}(10I_3, 0_{3 \times 3})$ —*i.e.*, positive weights on position outputs, zero weights on attitude outputs—and  $R = I_3$ . We let  $\hat{y}$  denote a circular trajectory in the  $xy$ -plane with radius 0.3; see Fig. 4 for an illustration. In addition, we choose  $\mathbb{U}$  and  $\mathbb{Y}$  in (3) such that the input is elementwise bounded within the interval  $[-1, 1]$ , the position output is bounded within the interval  $[-2, 2]$ ,  $[-2, 2]$ , and  $[0, 2]$  along the  $x$ -axis,  $y$ -axis, and  $z$ -axis, respectively; the attitude angle output is elementwise bounded within the interval  $[-\frac{\pi}{8}, \frac{\pi}{8}]$ .

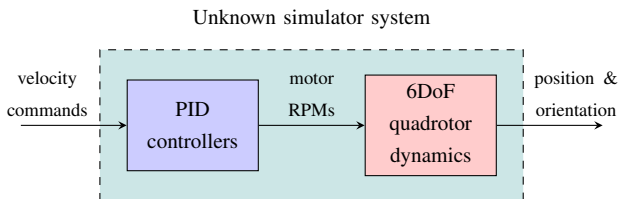


Fig. 2: The structure of the nonlinear system for quadrotor dynamics in the PyBullet simulator.

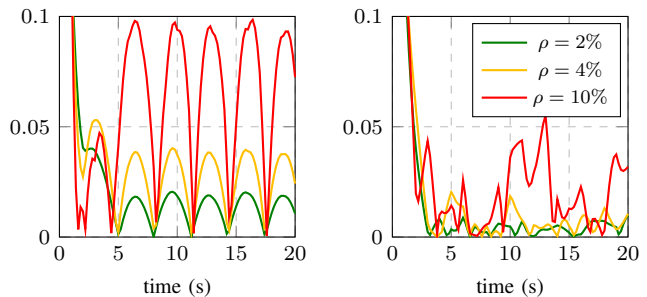
### B. Poisoning attacks setup

We construct the poisoning attack problem in (4) where function  $\psi(u)$  and set  $\mathbb{P}$  are chosen according to (5). For the oscillating masses system, we choose  $\tilde{u}$  to be sinusoidal signals with unit amplitude and unit angular frequency; for the PyBullet quadrotor system, we choose  $\tilde{u}$  to be a velocity command in the positive  $y$  direction.

### C. Numerical results

We demonstrate the output tracking error—the difference between the system’s output trajectory and the reference trajectory—of the oscillating masses system and PyBullet quadrotor system under different poisoning attacks in Fig. 3 and Fig. 4, respectively. These trajectories are simulated using the input optimized by solving (3) every 10 steps with attacks added to output data  $y_{ini}$ . As a benchmark in numerical experiments, we also consider random perturbation as  $p_{\text{rand}} = (\rho \|y_{ini}\| / \|v\|)v$  where each element in  $v \in \mathbb{R}^{\sigma n_v}$  is sampled independently from the standard Gaussian distribution. From these results, we can observe that: 1) compared with the linear oscillating masses, DPC is more sensitive to perturbation when applied to the nonlinear PyBullet quadrotor system, and 2) when applied to the PyBullet quadrotor system, the perturbations computed by Algorithm 1 increase the tracking error by more than ten times higher than those caused by random perturbations.

We also compare the efficiency of the implicit differentiation step used in Algorithm 1 against off-the-shelf software CVXPY layer [25] in terms of the dimension of the least squares problem—in Algorithm 1, this problem is solved when evaluating the pseudoinverse in line 3—they solve, which are summarized in Tab. I. These results show that, since we do not rely on homogeneous self-dual embedding, the size of the least-squares problem we solve in Algorithm 1—which equals  $2\ell(n_u + n_y) + \sigma n_u + n_g$ , *i.e.*, the number of equations in (9))—is less than half the size of the one solved in CVXPYlayers, which is around  $5\ell(n_u + n_y) + \sigma n_u + 2n_g$ , *i.e.*, the size of the homogeneous self-dual embedding (HSDE) for optimization (3)<sup>1</sup>.



(a) Perturbations via Alg. 1. (b) Random perturbations.

Fig. 3: The tracking error of the first mass’s displacement in the oscillating masses system.

TABLE I: The size of the least-squares problem solved when differentiating optimization (3).

Trajectory length $\ell$		25	50	100
Oscillating masses	CVXPY layer	1799	2549	4049
	Algorithm 1	<b>812</b>	<b>1112</b>	<b>1712</b>
PyBullet quadrotor	CVXPY layer	2192	3317	5567
	Algorithm 1	<b>968</b>	<b>1418</b>	<b>2318</b>

<sup>1</sup>Since CVXPYlayers introduce some internal auxiliary variables, the size of the HSDE is slightly higher than  $5\ell(n_u + n_y) + \sigma n_u + 2n_g$ .

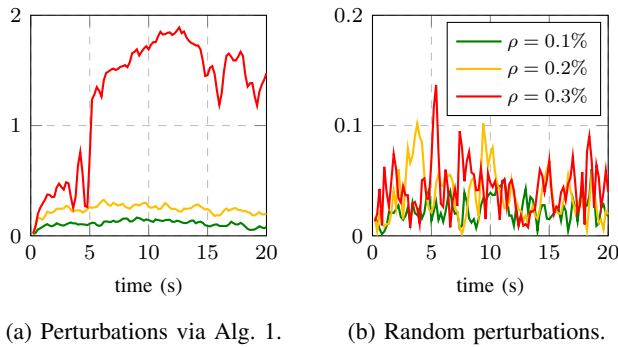


Fig. 4: The tracking error of the quadrotor position in PyBullet simulator.

## V. CONCLUSION

We study online poisoning attack problems in DPC. We develop an efficient numerical method to compute the data poisoning attacks based on implicit differentiation. Our future directions include attacks with partial knowledge of the parameters in DPC, as well as parameter design methods for DPC, where poisoning attacks act as a subroutine to evaluate the worst-case performance of any given parameter.

## REFERENCES

- [1] J. Coulson, J. Lygeros, and F. Dörfler, “Data-enabled predictive control: In the shallows of the deepc,” in *Proc. Eur. Control Conf.* IEEE, 2019, pp. 307–312.
- [2] A. Allibhoy and J. Cortés, “Data-based receding horizon control of linear network systems,” *IEEE Control Systems Letters*, vol. 5, no. 4, pp. 1207–1212, 2020.
- [3] F. Dörfler, J. Coulson, and I. Markovskiy, “Bridging direct & indirect data-driven control formulations via regularizations and relaxations,” *IEEE Trans. Autom. Control*, 2022.
- [4] J. C. Willems, P. Rapisarda, I. Markovskiy, and B. L. De Moor, “A note on persistency of excitation,” *Syst. Control Lett.*, vol. 54, no. 4, pp. 325–329, 2005.
- [5] H. J. van Waarde, C. De Persis, M. K. Camlibel, and P. Tesi, “Willems’ fundamental lemma for state-space systems and its extension to multiple datasets,” *IEEE Control Syst. Lett.*, vol. 4, no. 3, pp. 602–607, 2020.
- [6] Y. Yu, S. Talebi, H. J. van Waarde, U. Topcu, M. Mesbahi, and B. Açikmeşe, “On controllability and persistency of excitation in data-driven control: Extensions of Willems’ fundamental lemma,” in *Proc. IEEE Conf. Decision Control.* IEEE, 2021, pp. 6485–6490.
- [7] D. Q. Mayne, J. B. Rawlings, C. V. Rao, and P. O. Scokaert, “Constrained model predictive control: Stability and optimality,” *Automatica*, vol. 36, no. 6, pp. 789–814, 2000.
- [8] D. Q. Mayne, “Model predictive control: Recent developments and future promise,” *Automatica*, vol. 50, no. 12, pp. 2967–2986, 2014.
- [9] E. Elokda, J. Coulson, P. N. Beuchat, J. Lygeros, and F. Dörfler, “Data-enabled predictive control for quadcopters,” *Int. J. Robust Nonlinear Control*, vol. 31, no. 18, pp. 8916–8936, 2021.
- [10] L. Huang, J. Coulson, J. Lygeros, and F. Dörfler, “Decentralized data-enabled predictive control for power system oscillation damping,” *IEEE Trans Control Syst. Technol.*, vol. 30, no. 3, pp. 1065–1077, 2021.
- [11] V. Chinde, Y. Lin, and M. J. Ellis, “Data-enabled predictive control for building HVAC systems,” *J. Dyn. Syst. Meas. Control*, vol. 144, no. 8, p. 081001, 2022.
- [12] I. J. Goodfellow, J. Shlens, and C. Szegedy, “Explaining and harnessing adversarial examples,” *arXiv preprint arXiv:1412.6572 [stat.ML]*, 2014.
- [13] A. Kurakin, I. Goodfellow, and S. Bengio, “Adversarial machine learning at scale,” *arXiv preprint arXiv:1611.01236 [cs.CV]*, 2016.

- [14] P. Sharma, D. Austin, and H. Liu, “Attacks on machine learning: Adversarial examples in connected and autonomous vehicles,” in *Proc. IEEE Int. Symp. Technol. Homeland Secur.* IEEE, 2019, pp. 1–7.
- [15] S. Agarwal and S. Chinchali, “Task-driven data augmentation for vision-based robotic control,” in *Proc. Conf. Robot Learn. (to appear)*. PMLR, 2022.
- [16] D. Alpagó, F. Dörfler, and J. Lygeros, “An extended kalman filter for data-enabled predictive control,” *IEEE Control Syst. Lett.*, vol. 4, no. 4, pp. 994–999, 2020.
- [17] J. Coulson, J. Lygeros, and F. Dörfler, “Distributionally robust chance constrained data-enabled predictive control,” *IEEE Trans Autom. Control*, 2021.
- [18] M. Pajic, I. Lee, and G. J. Pappas, “Attack-resilient state estimation for noisy dynamical systems,” *IEEE Trans. Control Netw. Syst.*, vol. 4, no. 1, pp. 82–92, 2016.
- [19] F. Miao, Q. Zhu, M. Pajic, and G. J. Pappas, “Coding schemes for securing cyber-physical systems against stealthy data injection attacks,” *IEEE Trans. Control Netw. Syst.*, vol. 4, no. 1, pp. 106–117, 2016.
- [20] M. Pajic, J. Weimer, N. Bezzo, O. Sokolsky, G. J. Pappas, and I. Lee, “Design and implementation of attack-resilient cyberphysical systems: With a focus on attack-resilient state estimators,” *IEEE Control Syst. Mag.*, vol. 37, no. 2, pp. 66–81, 2017.
- [21] I. Jovanov and M. Pajic, “Relaxing integrity requirements for attack-resilient cyber-physical systems,” *IEEE Trans. Autom. Control*, vol. 64, no. 12, pp. 4843–4858, 2019.
- [22] A. Russo and A. Proutiere, “Poisoning attacks against data-driven control methods,” in *Proc. Amer. Control Conf.* IEEE, 2021, pp. 3234–3241.
- [23] A. Russo, M. Molinari, and A. Proutiere, “Data-driven control and data-poisoning attacks in buildings: the kth live-in lab case study,” in *Proc. Mediterranean Conf. Control Automat.* IEEE, 2021, pp. 53–58.
- [24] J. Panerati, H. Zheng, S. Zhou, J. Xu, A. Prorok, and A. P. Schoellig, “Learning to fly—a gym environment with PyBullet physics for reinforcement learning of multi-agent quadcopter control,” in *Proc. IEEE/RSJ Int. Conf. Intell. Robots Syst.* IEEE, 2021, pp. 7512–7519.
- [25] A. Agrawal, B. Amos, S. Barratt, S. Boyd, S. Diamond, and J. Z. Kolter, “Differentiable convex optimization layers,” *Adv. Neural Inf. Process. Syst.*, vol. 32, 2019.
- [26] J. Berberich, J. Köhler, M. A. Müller, and F. Allgöwer, “Data-driven model predictive control with stability and robustness guarantees,” *IEEE Trans. Autom. Control*, vol. 66, no. 4, pp. 1702–1717, 2020.
- [27] —, “Linear tracking mpc for nonlinear systems—part ii: The data-driven case,” *IEEE Trans. Autom. Control*, vol. 67, no. 9, pp. 4406–4421, 2022.
- [28] A. L. Dontchev and R. T. Rockafellar, *Implicit Functions and Solution Mappings: A View from Variational Analysis.* Springer, 2014.
- [29] H. H. Bauschke and P. L. Combettes, *Convex Analysis and Monotone Operator Theory in Hilbert Spaces.* Springer, 2017.
- [30] R. T. Rockafellar, *Convex Analysis.* Princeton University Press, 1970.
- [31] Y. Yu, P. Elango, and B. Açikmeşe, “Proportional-integral projected gradient method for model predictive control,” *IEEE Control Syst. Lett.*, vol. 5, no. 6, pp. 2174–2179, 2020.
- [32] Y. Yu, P. Elango, U. Topcu, and B. Açikmeşe, “Proportional–integral projected gradient method for conic optimization,” *Automatica*, vol. 142, p. 110359, 2022.
- [33] Y. Yu, P. Elango, B. Açikmeşe, and U. Topcu, “Extrapolated proportional-integral projected gradient method for conic optimization,” *IEEE Control Syst. Lett.*, vol. 7, pp. 73–78, 2023.
- [34] E. Busseti, W. M. Moursi, and S. Boyd, “Solution refinement at regular points of conic problems,” *Comput. Optim. Appl.*, vol. 74, no. 3, pp. 627–643, 2019.
- [35] H. H. Bauschke, “Projection algorithms and monotone operators,” Ph.D. dissertation, Theses (Dept. of Mathematics and Statistics)/Simon Fraser University, 1996.
- [36] J. F. Bard, *Practical bilevel optimization: algorithms and applications.* Springer Science & Business Media, 2013, vol. 30.
- [37] A. Domahidi, E. Chu, and S. Boyd, “ECOS: An SOCP solver for embedded systems,” in *Proc. Eur. Control Conf.* IEEE, 2013, pp. 3071–3076.